

Optimal Packet Scheduling in Energy Harvesting Multiple Access Channels with Common Data

Burhan Gulbahar, *Member, IEEE*

Abstract—Energy harvesting with the optimum power consumption and packet scheduling increase the lifetime and sustainability of the wireless sensor networks (WSNs) leading to green communications. Optimal packet scheduling solutions available for 2-user multiple-access channel (MAC) systems with energy harvesting transmitters do not consider the common data observed when collected sensor data is spatially or temporally correlated. Furthermore, the total received energy depends on the amount spent on the common data. In this paper, optimal packet scheduling for energy harvesting Gaussian MAC with common data is achieved by assuming the deterministic knowledge of the data and energy packets, i.e., offline solution, while also modelling the effect of the total received energy constraint. Optimum solution is achieved practically with a complex 3-level water filling algorithm. The algorithm is compared with the gradient descent search algorithm giving the global optimum solution. Furthermore, the capacity boundary region is numerically simulated by using water filling algorithm and the optimization results are compared for various points on the capacity boundary surface.

Index Terms—energy harvesting, MAC, common data, optimization, power.

I. INTRODUCTION

ENERGY harvesting with the optimum power adaptation and packet scheduling are significantly important for increasing the lifetime and sustainability of wireless sensor networks (WSNs) and for the green communications [1]–[4]. The scarcity and sporadic availability of the energy make it necessary the storage and the optimized utilization. Therefore, optimum energy management, data and energy transfer schemes are significantly important for WSNs.

Optimum packet scheduling in energy harvesting communication systems are achieved in various studies [5]–[9]. In [5], [6], algorithms for single-user energy harvesting communication systems are given. In [7], a directional water filling solution is given for the throughput maximization problem for a single-user fading channel with channel state information (CSI) feedback for energy harvesting finite capacity rechargeable batteries under offline and online knowledge. In [8], a two-hop relaying communication network with energy harvesting rechargeable nodes is optimized. In [9], energy usage is minimized over a wireless channel via changing packet transmission times.

The optimization for MAC schemes are achieved in [1], [2], [10]. Optimal packet scheduling is given for a 2-user MAC with energy harvesting transmitters and deterministic

assumption of the data and energy packets, i.e., offline solution. In [11], the capacity region of the energy harvesting Gaussian MAC is analysed with one-way energy transfer capability while in [12], the capacity is analysed with amplitude constraints and batteryless energy harvesting transmitters. In [3], optimal continuous-time online power policies, in [13], utility maximization framework modelling using a water filling approach and in [4], the effect of storage losses are incorporated. However, these studies do not consider Gaussian MAC with common data in a capacity boundary and throughput maximization analysis and optimum scheduling framework.

Besides that, WSNs collect common data having the spatial or temporal correlation and the correlation is exploited to save the resources [14], [15]. The capacity region in a Gaussian MAC channel with common data and optimum power allocation is characterized in [16] while in [17], similar analyses are achieved for the discrete p-transmitter/q-receiver MAC with a common message. In [18], combination with joint source-channel codes and optimal policies through a memoryless fading MAC are given. In [19], the 2-user Gaussian MAC with common message (MACCM) and with conferencing encoders (MACCE) are analysed. However, there is no study combining the optimum scheduling in a Gaussian MAC with common data in an energy harvesting communication system.

On the other hand, combined data and energy transfer is utilized in energy harvesting systems. In [20], MAC with received energy constraint is analysed showing the trade-off between the data rate and the received energy. In [21], a two-way communication system is considered. In [22], MAC and two way channels with energy harvesting and cooperating transmitters are analyzed. In [23], the energy harvesting MAC relay with bidirectional energy transfer leads to a directional water filling solution. However, there is no study combining optimum scheduling and energy harvesting with received energy constraint in a Gaussian MAC with common data.

To the best of our knowledge, in this work, optimum offline packet scheduling and power policy is, for the first time, modelled, solved and leaded with the unique water filling solution in a Gaussian MAC with common data scheme. Furthermore, the modelling of the problem includes, for the first time, the constraint of the total received energy. The Karush-Kuhn-Tucker (KKT) solution is, for the first time, given for optimum packet scheduling power policy for energy harvesting transmitters in a Gaussian MAC with common data scheme. The 3-level unique water filling algorithm is, for the first time, introduced. The optimality of the water filling algorithm is shown by comparing with the gradient search iterative algorithm in a numerical simulation study. The capacity boundary region for the rates of the individual

B. Gulbahar is with VESTEL Electronics Research Department, Organize Sanayi Bölgesi, Manisa, Turkey 45030 and an adjunct faculty member in the Department of Electrical and Electronics Engineering, Özyeğin University, İstanbul, Turkey 34794. e-mail: burhan.gulbahar@vestel.com.tr, burhan.gulbahar@ozyegin.edu.tr.

and the common data messages is numerically simulated with the optimum solution. The optimum packet scheduling and power consumption profiles are compared by choosing various points on the surface of the capacity boundary. However, in simulation studies the total transmitted energy constraint is not taken into account and left as a future work.

The remainder of the paper is organized as the following. In Section II, related work on optimum power allocation policies in energy harvesting communication systems are explored. In Section III, the system model for the Gaussian MAC with common data is defined. Then, in Section IV, data throughput maximization problem is defined, KKT solution, the water filling and iterative gradient descent algorithms are presented. In Section V, a simulation study is performed illustrating optimum scheduling, capacity boundary and the comparison of two algorithms. Finally, in Section VI, the conclusions are given and future works are pointed out.

II. RELATED WORK

Optimum online and offline packet scheduling in energy harvesting communication systems are recently investigated for single hop, MAC and broadcast systems recently.

In [7], a directional water filling optimizes the throughput maximization problem for a single-user fading channel with additive Gaussian noise with finite capacity rechargeable batteries under offline and online knowledge. Optimal packet scheduling for single-user energy harvesting communication systems are presented in [5], [6]. In [8], a two-hop relaying communication network with energy harvesting rechargeable nodes is formulated for the offline end-to-end throughput maximization as a convex optimization problem. In [9], the energy used by a node in a wireless communication network is minimized for the packets to be sent in a given amount of time by varying packet transmission times and power levels by considering both optimum offline and online scheduling.

The similar analyses are achieved for MAC schemes. In [11], the capacity region of the energy harvesting Gaussian MAC is analyzed with one-way energy transfer capability. In [1], [2], [10], optimal packet scheduling problem is solved in a 2-user MAC system with energy harvesting transmitters where the energy harvesting times and harvested energy amounts are known before the transmission. KKT solution and the generalized iterative backward water filling algorithm are presented. In [12], the capacity region of Gaussian MAC with amplitude constraints and batteryless energy harvesting transmitters are analysed. In [3], optimal continuous-time online power policies for energy harvesting MACs are presented. In [13], energy harvesting transmitter and receiver pair is considered in a utility maximization framework achieving power policy using a water filling approach. In [4], optimal transmit power policy for energy harvesting transmitters in a Gaussian MAC is presented by also considering storage losses. However, these studies do not consider the common data in an optimum scheduling and power adaptation framework and do not propose the unique water filling solution obtained when considering common data and also energy transfer.

On the other hand, data correlation in WSNs are significantly important which are exploited to save the power-

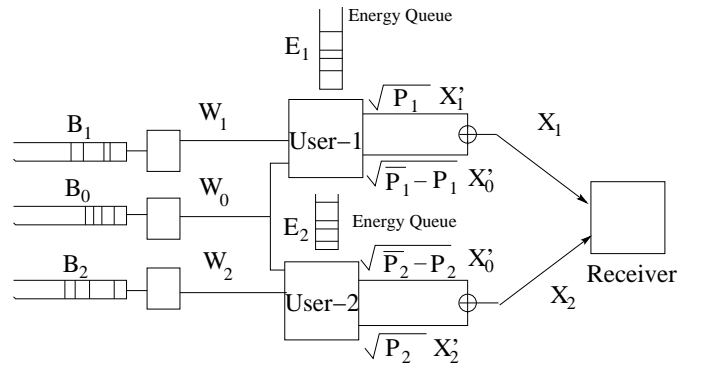


Fig. 1. System model for Gaussian MAC with common data and energy harvesting transmitters.

bandwidth resources [14], [15]. In [16], the explicit characterization of the capacity region in a Gaussian MAC channel with common data and fading is considered. The optimum power allocation schemes that achieve arbitrary rate tuples on the boundary of the capacity region are presented and numerically computed. In [17], the capacity region of the discrete p-transmitter/q-receiver MAC coined as General MAC (GMAC) with a common message is derived. In [18], information-theoretic results and power allocation policies in combination with joint source-channel codes on the transmission of memoryless dependent sources through a memoryless fading MAC are analysed. In [19], 2-user MACCM and MACCE with CSI are analyzed. The capacity results for the Gaussian MAC with cooperative encoders and with additive interference known non-causally to both encoders are presented. However, none of these studies combine energy harvesting, optimum scheduling of transmissions and power adaptation, data rate maximization and modelling of the optimum solution including energy transfer in a Gaussian fading MAC with common data.

The optimization of both data and energy transfer at the same channel in a Gaussian MAC scheme is considered in various works. In [20], MAC with received energy constraint is analysed showing achievable trade-off between the data rate and the received energy. In [21], a two-way communication system is considered where the energy used for communication is recycled. In [22], MAC and two way channels with energy harvesting and energy cooperating transmitters are analysed for jointly optimal transmit power allocation and energy transfer policies achieving the sum-capacity. In [23], the energy harvesting multiple access relay channel with bidirectional energy transfer is optimized for the sum rate and a directional water filling solution is proposed. However, none of these studies combine common data in a Gaussian MAC, gives the optimum solution for the capacity boundary in an offline scheduling framework.

III. SYSTEM MODEL

In this paper, the Gaussian MAC has two transmitters and one receiver as shown in Fig.1 where the components of the system model are seen [1], [2], [16].

Each user has their individual data packets and also a common message known by both transmitters. It is assumed

that energy harvesting amounts and the times are known. Similar to [1], [2], energy harvesting times are put in ascending order and the length of the time interval between two energy harvesting instants t_n and t_{n+1} is denoted by $L(n)$. For example, 1st user harvests $E_1(n)$ at the time instant t_n and 2nd user harvests $E_2(n+1)$ at the time instant t_{n+1} . The users do not change the data rate in these intervals. The capacity or the data rate in a time interval L with the total power P is denoted by $C(P)$ and given by the following,

$$C(P) = W_{Tot} \log \left(1 + \frac{P}{A} \right) L \quad (1)$$

where W_{Tot} refers the total bandwidth and the constant A equals to $N_0 W_{Tot} / h$ where N_0 is the noise spectral density and h is the fixed path loss.

In this article, we assume offline solution [2]. Data packets are available at the start of each time interval, the harvested energy is stored in sensor nodes and the fading is constant and known previously. The target is to find the maximum data throughput regions for the three kinds of user data for any given deadline time T_f and propose a water filling algorithm finding the optimal solution.

We can model the Gaussian MAC as the following,

$$X_i = \sqrt{P_i} X'_i + \sqrt{\overline{P_i} - P_i} X'_0, \quad i \in [1, 2] \quad (2)$$

$$Y = H_1 X_1 + H_2 X_2 + Z, \quad Z \sim N(0, 1) \quad (3)$$

$$= h \left(\sqrt{P_1} X'_1 + \sqrt{P_2} X'_2 + \sqrt{P_0} X'_0 \right) + Z \quad (4)$$

where we assume that the fading is $H_1 = H_2 = h$ and unity throughout the formulation. The power of the correlated information can be found as $P_0 = \left(\sqrt{\overline{P_1} - P_1} + \sqrt{\overline{P_2} - P_2} \right)^2$. A constant $0 \leq \rho \leq 1$ is defined such that $\overline{P_1} = P_1 + \rho^2 P_0$ and $\overline{P_2} = P_2 + (1 - \rho)^2 P_0$. Three independent messages are W_0 , W_1 and W_2 where W_0 is known by both the users. The capacity region with the common data is the following [16],

$$R_1 \leq C(P_1); \quad R_2 \leq C(P_2); \quad R_1 + R_2 \leq C(P_1 + P_2) \quad (5)$$

$$R_1 + R_2 + R_0 \leq C(P_1 + P_2 + P_0) \quad (6)$$

where $0 \leq P_1 \leq \overline{P_1}$, $0 \leq P_2 \leq \overline{P_2}$ and $P_0 = \left(\sqrt{\overline{P_1} - P_1} + \sqrt{\overline{P_2} - P_2} \right)^2$. The capacity region $B(P_1, P_2)$ can be observed in Fig.2 for some specific $P_1 \leq \overline{P_1}$ and $P_2 \leq \overline{P_2}$. This region will be valid for both single time interval and for the overall capacity region throughout the energy harvesting process. The important boundary points on the curve are as the following [16],

$$Q = (0, 0, C(P_{0,2}^s)); \quad S = (C(P_1), 0, C(P_{0,2}^s) - C(P_1)) \quad (7)$$

$$T = (C(P_1), C(P_{1,2}^s) - C(P_1), C(P_{0,2}^s) - C(P_{1,2}^s)) \quad (8)$$

where $P_{0,2}^s = P_0 + P_1 + P_2$, $P_{1,2}^s = P_1 + P_2$. The points V and U can be obtained in the same manner with S and T by changing the roles of the user 1 and 2. It is proved in [16] that all the points on the capacity region of Gaussian MAC can be achieved by some point on the line segment $T - U$ of $B(P_1, P_2)$ for some $0 \leq P_1 \leq \overline{P_1}$, $0 \leq P_2 \leq \overline{P_2}$ and are the union of $C(\overline{P_1}, \overline{P_2}) = \bigcup_{\mathbf{P}, \rho \in F} C_f(\mathbf{P}, \rho)$ where $C_f(\mathbf{P}, \rho)$ is

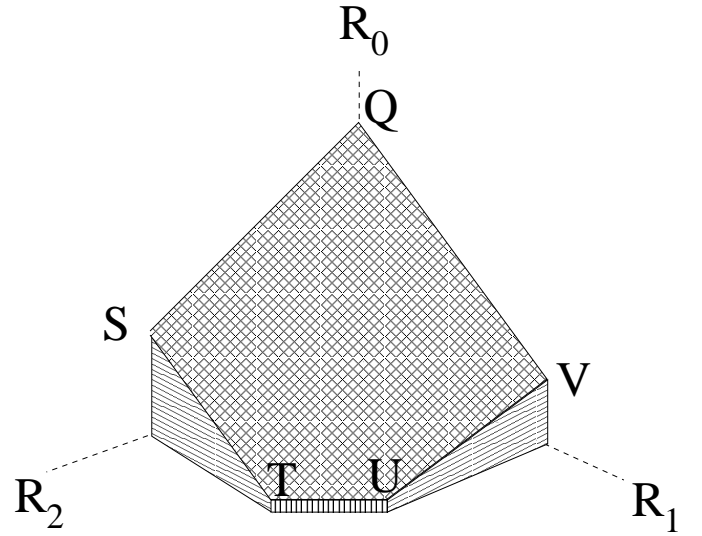


Fig. 2. Illustrative capacity region of Gaussian MAC with common data.

the set of R_1, R_2, R_0 in (5) and the set F is the following,

$$F = \left\{ (\mathbf{P}, \rho) : \begin{aligned} &P_0, P_1, P_2 \geq 0, 0 \leq \rho \leq 1, \\ &P_1 + \rho^2 P_0 \leq \overline{P_1}, P_2 + \rho^2 P_0 \leq \overline{P_2} \end{aligned} \right\} \quad (9)$$

It is stressed out that the boundary surface of $C(\overline{P_1}, \overline{P_2})$ can be found with the following optimization problem which will be used throughout the paper,

$$\max_{\mathbf{R}, \mathbf{P}, \rho} \mu_1 R_1 + \mu_2 R_2 + \mu_0 R_0 \quad \text{s.t.} \quad \mathbf{R} \in C_f(\mathbf{P}, \rho) \quad (10)$$

Since $C_f(\mathbf{P}, \rho)$ has a capacity boundary surface as in Fig.2, we can find Q, S and T points by using (7 - 8). V and U can be found by swapping the roles of two users. It is observed that for various μ values, various boundary points maximize $C(\overline{P_1}, \overline{P_2})$ as in the following,

$$\mu_0 \geq \max(\mu_1, \mu_2) \rightarrow Q; \quad \mu_1 \geq \mu_2 \geq \mu_0 \rightarrow T \quad (11)$$

$$\mu_1 \geq \mu_0 \geq \mu_2 \rightarrow S; \quad \mu_2 \geq \mu_1 \geq \mu_0 \rightarrow U \quad (12)$$

$$\mu_2 \geq \mu_0 \geq \mu_1 \rightarrow V \quad (13)$$

where $U : (C(P_{1,2}^s) - C(P_2), C(P_2), C(P_{0,2}^s) - C(P_{1,2}^s))$ and $V : (0, C(P_2), C(P_{0,2}^s) - C(P_2))$. It is known that $C_f(\mathbf{P}, \rho)$ is a convex region [2], [11], [16] leading to convex solution of the optimal offline scheduling capacity. Then, based on the optimization method for a single time interval in [16], the optimal scheduling will be achieved which maximizes the overall capacity region for some specific energy harvesting scenario. The overall capacity of a number of time intervals is found by summing the capacities in each time interval similar to the MAC scheduling framework in [2] where no common data is assumed. Then, the points on the capacity or the maximum data throughput will be obtained by changing $\mu_{1,2,3}$ and maximizing $C(\overline{P_1}, \overline{P_2})$.

IV. DATA THROUGHPUT MAXIMIZATION AND OPTIMUM POWER POLICY

The points on the 3-D capacity curve of R_0, R_1, R_2 are found by using the cases $\mu_1 \geq \mu_2 \geq \mu_0$, $\mu_1 \geq \mu_0 \geq \mu_2$, $\mu_0 \geq \max(\mu_1, \mu_2)$ for the half part of the curve [16]. The other half part can be found by changing the roles of the nodes and μ_1 and μ_2 . Firstly, the optimization problem is defined, then, KKT conditions are written similar to the study in [2] with the difference of the incorporation of the common data and the constraint for the total received energy. Then, the water filling algorithm for the KKT solution will be presented. The iterative gradient descent algorithm gives the global solution and it is compared with the water filling algorithm.

A. Capacity Maximization Problem

Optimization problem is defined for three different rate tuples given in (11- 12) [2], [16].

1) $\mu_1 \geq \mu_2 \geq \mu_0$:

$$\max \sum_{k=1}^3 \text{OF}_{1,k} \quad (14)$$

s.t. positive power and the sharing constraint for P_0 ,

$$P_1(n), P_2(n), P_0(n) \geq 0, 0 \leq \rho(n) \leq 1; 1 \leq n \leq N \quad (15)$$

causality constraints for the the total energy,

$$\sum_{n=1}^N \overline{P}_1(n)L(n) - E_1^{T,1} = 0; \sum_{n=1}^N \overline{P}_2(n)L(n) - E_2^{T,1} = 0 \quad (16)$$

where $\overline{P}_1(n) = P_1(n) + \rho_n^2 P_0(n)$, $\overline{P}_2(n) = P_2(n) + (1 - \rho(n))^2 P_0(n)$, $E_j^{T,i} = \sum_{n=i-1}^{N-1} E_{j,n}$ for $j = [1, 2]$, for the consumed energies in the time interval $[i, N]$ for $i \geq 2$,

$$-\sum_{n=i}^N \overline{P}_1(n)L(n) + E_1^{T,i} \leq 0; -\sum_{n=i}^N \overline{P}_2(n)L(n) + E_2^{T,i} \leq 0 \quad (17)$$

and the total received power constraint,

$$-\sum_{n=1}^N \rho(n)(1 - \rho(n))P_0(n)L(n) + E_{th} \leq 0 \quad (18)$$

where objective function (OF) for the point T is following,

$$\text{OF}_{1,1} = -\mu_0 \sum_{n=1}^N C(P_0(n) + P_1(n) + P_2(n)) \quad (19)$$

$$\text{OF}_{1,2} = -(\mu_2 - \mu_0) \sum_{n=1}^N C(P_1(n) + P_2(n)) \quad (20)$$

$$\text{OF}_{1,3} = -(\mu_1 - \mu_2) \sum_{n=1}^N C(P_1(n)) \quad (21)$$

(16 - 17) include the causality constraints such that the consumed energy from the time t_i to t_N , i.e., $\sum_{n=1}^N (P_1(n) + \rho_n^2 P_0(n))L(n)$, is larger than the total harvested energy in that interval, i.e., $E_1^{T,i}$, assuming that the energy stored and harvested before t_i can be used. (18) is the constraint for the

total received power obtained using (16) as follows,

$$\begin{aligned} \sum_{n=i}^N (P_1(n) + P_2(n) + P_0(n))L(n) &\geq E_{Targ} \\ E_{Tot} - 2 \sum_{n=1}^N \rho(n)(\rho(n) - 1)P_0(n)L(n) &\geq E_{Targ} \\ - \sum_{n=1}^N \rho(n)(1 - \rho(n))P_0(n)L(n) &\leq -E_{th} \end{aligned} \quad (22)$$

where E_{Targ} is the targeted total received power, $E_{Tot} = \sum_{n=0}^{N-1} (E_{1,n} + E_{2,n})$ is the total harvested energy and $E_{th} \triangleq (E_{Targ} - E_{Tot}) / 2$.

2) $\mu_1 \geq \mu_0 \geq \mu_2$: The constraints will be similar to the first case except P_2 will be set to zero. In this case, the sum $\sum_{k=1}^2 \text{OF}_{2,k}$ coming from the point S in (12) maximizes the capacity and P_2 is equal to zero throughout the optimization. Therefore by equalizing P_2 equal to zero in (15 - 21), the optimization problem can be achieved not written in explicit detail. $\text{OF}_{2,1}$ and $\text{OF}_{2,2}$ are defined as follows,

$$\text{OF}_{2,1} = -\mu_0 C(P_0(n) + P_1(n)) \quad (23)$$

$$\text{OF}_{2,2} = -(\mu_1 - \mu_0)C(P_1(n)) \quad (24)$$

3) $\mu_0 \geq \max(\mu_1, \mu_2)$: In this case, $\text{OF}_{3,1}$ coming from the point Q in (11) maximizes the capacity. Therefore, in the optimum solution, P_1 and P_2 will be zero and all the power will be consumed for the common data. $\text{OF}_{3,1}$ is defined as $\text{OF}_{3,1} = -\mu_0 C(P_0(n))$

B. Karush-Kuhn Tucker Solution

Maximization problems are solved by using KKT multipliers for 3 different cases [1], [2]. Since $C_f(\mathbf{P}, \rho)$ or the summation of OFs lead to convex solution [16] for a single time interval and the maximum departure region obtained for a set of time intervals in a Gaussian MAC setting leads to convex solution for the optimal offline scheduling capacity [2], KKT solution will also lead to unique global optimum.

1) $\mu_1 \geq \mu_2 \geq \mu_0$:

$$\max \sum_{k=1}^{10} \text{OF}_{1,k} \quad (25)$$

s.t. KKT multipliers are positive or zero,

$$\lambda_{m,n} \geq 0, n \in [2, N], m \in [1, 2]; \quad (26)$$

$$\lambda_{m,n} \geq 0, n \in [1, N], m \in [3, 8] \quad (27)$$

positive power constraints and the constraint for P_0 and ρ in (15), causality constraints for the harvested and consumed energies in (16) for the total energies,

$$\lambda_{1,1} \left(-\sum_{n=1}^N \overline{P}_1(n)L(n) + E_1^{T,1} \right) = 0 \quad (28)$$

$$\lambda_{2,1} \left(-\sum_{n=1}^N \overline{P}_2(n)L(n) + E_1^{T,2} \right) = 0 \quad (29)$$

and for the consumed energies in the time interval $[i, N]$, $i \in [2, N]$

$$\lambda_{1,i} \left(-\sum_{n=i}^N \overline{P_1}(n)L(n) + \sum_{n=i-1}^{N-1} E_{1,n} \right) = 0 \quad (30)$$

$$\lambda_{2,i} \left(-\sum_{n=i}^N \overline{P_2}(n)L(n) + \sum_{n=i-1}^{N-1} E_{2,n} \right) = 0 \quad (31)$$

the multiplications of KKT multipliers with the inequalities in (15) for $i \in [2, N]$,

$$\lambda_{3,n}\rho_n = \lambda_{4,n}(\rho_n - 1) = \lambda_{5,n}P_1(n) = 0 \quad (32)$$

$$\lambda_{6,n}P_2(n) = \lambda_{7,n}P_0(n) = 0 \quad (33)$$

and the total received power constraint,

$$\lambda_8 \left(-\sum_{n=1}^N \rho(n)(1 - \rho(n))P_0(n)L(n) + E_{th} \right) = 0 \quad (34)$$

where the components of OF corresponding to the point T are defined in (19 -21). The ones for the causality constraints is,

$$\text{OF}_{1,m} = \sum_{i=2}^N \left[\lambda_{k,i} \left(-\sum_{n=i}^N \overline{P_k}(n)L(n) + E_k^{T,i} \right) \right] \quad (35)$$

where $[k, m] = [1, 4]$ or $[2, 5]$, the ones regarding (32-33) is,

$$\text{OF}_{1,6} = L(n) \left(\sum_{n=1}^N \lambda_{3,n}(-\rho_n) + \sum_{n=1}^N \lambda_{4,n}(\rho_n - 1) \right) \quad (36)$$

$$\begin{aligned} \text{OF}_{1,7} = & -\left(\sum_{n=1}^N \lambda_{5,n}P_1(n) + \sum_{n=1}^N \lambda_{6,n}P_2(n) \right. \\ & \left. + \sum_{n=1}^N \lambda_{7,n}P_0(n) \right) L(n) \end{aligned} \quad (37)$$

regarding the total received power constraint,

$$\text{OF}_{1,8} = \lambda_8 \left(-\sum_{n=1}^N \rho(n)(1 - \rho(n))P_0(n)L(n) + E_{th} \right) \quad (38)$$

and the ones for the total consumed and the harvested power,

$$\text{OF}_{1,m} = \lambda_{k,1} \left(-\sum_{n=1}^N \overline{P_k}(n)L(n) + E_1^{T,k} \right) \quad (39)$$

where $[k, m] = [1, 9]$ or $[2, 10]$. Taking the derivative with respect to $P_1(n)$, $P_2(n)$, $P_0(n)$, $\rho(n)$ and equalizing to zero give the following KKT equalities for $j \in [1, N]$,

$$\begin{aligned} P_{1,j} : & \frac{\mu'_0}{1 + P'_0(j) + P'_1(j) + P'_2(j)} + \frac{\mu'_2 - \mu'_0}{1 + P'_1(j) + P'_2(j)} \\ & + \frac{\mu'_1 - \mu'_2}{1 + P'_1(j)} = \lambda_{1,j}^p - \lambda_{5,j} \end{aligned} \quad (40)$$

$$\begin{aligned} P_{2,j} : & \frac{\mu'_0}{1 + P'_0(j) + P'_1(j) + P'_2(j)} + \frac{\mu'_2 - \mu'_0}{1 + P'_1(j) + P'_2(j)} \\ & = \lambda_{2,j}^p - \lambda_{6,j} \end{aligned} \quad (41)$$

$$\begin{aligned} P_{0,j} : & \frac{\mu'_0}{1 + P'_0(j) + P'_1(j) + P'_2(j)} = \\ & \lambda_{1,j}^p \rho_j^2 + \lambda_{2,j}^p (1 - \rho_j)^2 - \lambda_{7,j} - \lambda_8 (1 - \rho_j) \rho_j \quad (42) \\ \rho_j : & P'_0(j) [\rho_j (2\lambda_{1,j}^p + 2\lambda_{2,j}^p + 2\lambda_8)] \\ & = P'_0(j) [2\lambda_{2,j}^p + \lambda_8] + \frac{\lambda_{3,j} - \lambda_{4,j}}{A} \end{aligned} \quad (43)$$

where $\lambda_{m,j}^p = \lambda_{1,1} - \sum_{i=2}^j \lambda_{m,i}$ with $m = [1, 2]$, $\mu'_i = \mu_i W_{Tot} / A$, $P'_0(j) = P_0(j) / A$. If $0 < \rho_j < 1$, the following can be obtained,

$$\rho_j = \frac{2\lambda_{2,j}^p + \lambda_8}{2\lambda_{2,j}^p + 2\lambda_{1,j}^p + 2\lambda_8} \quad (44)$$

Putting into 42, the equation becomes as the following,

$$P_{0,j} : \frac{\mu'_0}{1 + P'_0(j) + P'_1(j) + P'_2(j)} = g(\lambda_{1,j}^p, \lambda_{2,j}^p, \lambda_8) - \lambda_{7,j} \quad (45)$$

where $g(\lambda_{1,j}^p, \lambda_{2,j}^p, \lambda_8)$ is defined as

$$g(\lambda_{1,j}^p, \lambda_{2,j}^p, \lambda_8) \triangleq \frac{4\lambda_{1,j}^p \lambda_{2,j}^p - \lambda_8^2}{4(\lambda_{1,j}^p + \lambda_{2,j}^p + \lambda_8)} \quad (46)$$

The KKT multiplier regions for the single time interval can be found with a similar approach in [16] and are given in Appendix-A. The total transmitted energy constraint is also added to the formulas as different from the version in [16].

The constraints and the components of the objective functions for the other 2 cases are found with a similar approach to the case 1. Therefore, in the following, only the final expressions will be presented without the detailed explanation.

2) $\mu_1 \geq \mu_0 \geq \mu_2$: Similar to the approach performed for the case-1 and taking the derivative with respect to $P_1(n)$, $P_0(n)$, $\rho(n)$ gives the following for $j \in [1, N]$,

$$\begin{aligned} P_{1,j} : & \frac{\mu'_0}{1 + P'_0(j) + P'_1(j)} + \frac{\mu'_1 - \mu'_0}{1 + P'_1(j)} \\ & = \lambda_{1,j}^p - \lambda_{5,j} \end{aligned} \quad (47)$$

$$\begin{aligned} P_{0,j} : & \frac{\mu'_0}{1 + P'_0(j) + P'_1(j)} = \\ & \lambda_{1,j}^p \rho_j^2 + \lambda_{2,j}^p (1 - \rho_j)^2 - \lambda_{7,j} - \lambda_8 (1 - \rho_j) \rho_j \quad (48) \\ \rho_j : & P'_0(j) [\rho_j (2\lambda_{1,j}^p + 2\lambda_{2,j}^p + 2\lambda_8)] \\ & = P'_0(j) [2\lambda_{2,j}^p + \lambda_8] + \frac{\lambda_{3,j} - \lambda_{4,j}}{A} \end{aligned} \quad (49)$$

If $0 < \rho_j < 1$, the following can be obtained,

$$\rho_j = \frac{2\lambda_{2,j}^p + \lambda_8}{2\lambda_{2,j}^p + 2\lambda_{1,j}^p + 2\lambda_8} \quad (50)$$

Putting into 48, the equation becomes as the following,

$$P_{0,j} : \frac{\mu'_0}{1 + P'_0(j) + P'_1(j)} = g(\lambda_{1,j}^p, \lambda_{2,j}^p, \lambda_8) - \lambda_{7,j} \quad (51)$$

3) $\mu_0 \geq \max(\mu_1, \mu_2)$: After defining the optimization problem and similarly taking the derivative with respect to $P_0(n)$, $\rho(n)$, equalization to zero gives the following KKT

equalities for $j \in [1, N]$,

$$P_{0,j} : \frac{\mu_0}{1 + P_0'(j)} = g(\lambda_{1,j}^p, \lambda_{2,j}^p, \lambda_8) \quad (52)$$

$$= \lambda_{1,j}^p \rho_j^2 + \lambda_{2,j}^p (1 - \rho_j)^2 - \lambda_8 (1 - \rho_j) \rho_j \quad (53)$$

$$\rho_j : \rho_j = \frac{2\lambda_{2,j}^p + \lambda_8}{2\lambda_{2,j}^p + 2\lambda_{1,j}^p + 2\lambda_8} \quad (54)$$

Now, the water filling algorithm satisfying KKT solutions will be developed.

C. Optimal Water filling Algorithm

The water filling algorithm has the similar structure for different constant multiplier μ values but with different number of water levels and types. Therefore, the case for $\mu_1 \geq \mu_2 \geq \mu_0$ is analysed and explained as an illustrative example. The case for the single time epoch leads to 8 different regions defined with respect to the KKT multipliers [16]. In a correlated setting, different from the previous studies [1], [2], there will be comparison of two time intervals where each one is optimized with respect to the current total energy and in different regions of KKT multipliers.

When one of the nodes, e.g., first node, transmits energy from the time step j to the next time step $j + 1$, then the corresponding KKT multiplier in (30, 31) becomes zero and the equality $\lambda_{1,j}^p = \lambda_{1,j+1}^p$ is satisfied. On the other hand, if the optimum scheduling includes no energy transfer from some node then $\lambda_{1,j}^p \geq \lambda_{1,j+1}^p$ should be satisfied. Therefore, in the algorithm, at each time step, both of the nodes are experimented one by one to transmit energy and whether the water-level equalities/inequalities and the corresponding equalities/inequalities for $\lambda_{1,j}^p, \lambda_{1,j+1}^p, \lambda_{2,j}^p, \lambda_{2,j+1}^p$, are satisfied based on the regions of two time steps shown in the Tables II in Appendix-B. For example, if 1st user is chosen in a time step- j to transmit energy to the next time step as a possible candidate of optimum solution, and assume that the region in time step- j is 5 and the region in the time step- $j + 1$ is 2, then, based on Table-II and $\lambda_{1,j}^p = \lambda_{1,j+1}^p$, the following should be satisfied if the transfer leads to the optimum solution,

$$W_1(j) = \lambda_{1,j}^p \geq W_1(j + 1) = \lambda_{1,j}^p - \lambda_{5,j+1} \quad (55)$$

$$W_2(j) = \lambda_{2,j}^p - \lambda_{6,j} \leq W_2(j + 1) = \lambda_{2,j+1}^p - \lambda_{6,j+1} \quad (56)$$

$$W_3(j) \geq W_3(j + 1) \quad (57)$$

$$\lambda_{1,j}^p = \lambda_{1,j+1}^p; \quad \lambda_{2,j}^p \geq \lambda_{2,j+1}^p \quad (58)$$

where $W_3(j) = g(\lambda_{1,j}^p, \lambda_{2,j}^p, \lambda_8)$ and $W_3(j + 1) = g(\lambda_{1,j+1}^p, \lambda_{2,j+1}^p, \lambda_8)$. Then, by looking at the difference between water levels and using an iterative weighted search algorithm, water levels are optimized. The comparison tables regarding the water levels can be seen in Tables III and IV in Appendix-B. Here, similar to [1], [2], [10], an iterative backward water filling procedure is applied as shown in Algorithm-1. The water filling algorithm checks the energy transfer for both of the levels in a more complicated manner compared with the previous versions where one of the nodes is assumed to have fixed scheduling. Since the correlated power also depends on the power profile of both users in equalizing water levels, here both of the nodes are optimized at the same

Algorithm 1: Water filling Algorithm

```

while Water levels are not equalized do
  for all  $n = N$  to 2 do
    Optimize the  $P_0(n), P_1(n), P_2(n)$  and  $P_0(n - 1), P_1(n - 1), P_2(n - 1)$  using the single time interval regions and the solutions in Appendix-A at time steps  $n$  and  $n - 1$  individually
    Find the resulting KKT multiplier  $\lambda$  values, water levels at time intervals  $n$  and  $n - 1$ 
  if Water levels and  $\lambda$  values are not in equilibrium then
    if  $E_1(n)/L(n) \geq E_1(n - 1)/L(n - 1)$  AND  $E_2(n)/L(n) \geq E_2(n - 1)/L(n - 1)$  then
      Send energy from both the nodes from the time interval  $n - 1$  to  $n$  until  $E_{1,2}(n)/L(n) = E_{1,2}(n - 1)/L(n - 1)$ 
    else
      Send energy only from the first node from the time interval  $n - 1$  to  $n$  and check whether it satisfies the optimum water filling
      Send energy only from the second node from the time interval  $n - 1$  to  $n$  and check whether it satisfies the optimum water filling
      Choose the optimum energy sharing for either of the nodes satisfying water-level equalization and mark the energy transfer at that time interval for that specific node for the future energy transfers
    end if
  end if
end for
end while

```

time. Now, the gradient descent algorithm is introduced which will be a comparison test-bed for the water filling solution as an algorithm converging to the global maximum.

D. Iterative Gradient Descent Algorithm

It is known that $C_f(\mathbf{P}, \rho)$ is a convex region [2], [11], [16]. Global solution is found by iterative gradient search by optimizing the scheduling for the first node with the other fixed, then, the reverse is applied. The iterative nature of the water filling algorithm in [2] is shown to converge to the global optimum. Therefore, the same iterative technique is applied in this article. The optimization continues iteratively, until the overall data throughput increase after each iteration is below some threshold. Assuming N time steps, firstly, the gradient of the overall throughput $C(\mathbf{E})$ is found as the following,

$$\nabla C(\mathbf{E}) = \left[\frac{\partial C(\mathbf{E})}{\partial E_{1,1}}, \frac{\partial C(\mathbf{E})}{\partial E_{1,2}}, \dots, \frac{\partial C(\mathbf{E})}{\partial E_{2,N}} \right]^T \quad (59)$$

where the partial derivatives are found as the following, e.g., for the first node,

$$\frac{\partial C(\mathbf{E})}{\partial E_{1,n}} = \frac{C(E_{1,1}, \dots, E_{1,n} + \Delta E, \dots, E_{2,N}) - C(\mathbf{E})}{\Delta E} \quad (60)$$

and $\mathbf{E} = [E_{1,1}, E_{1,2}, \dots, E_{1,N}, E_{2,1}, E_{2,2}, \dots, E_{2,N}]^T$ is the available energy at each time step for each node. The direction maximizing the gradient is found by computing the directional derivative for all the possible energy scheduling cases for the chosen node at the current iteration. The possible energy scheduling cases $d_s = [d_1, d_2, \dots, d_N]^T$ are found by finding all the combinations of the rows of the matrix D of dimension $N \times N$ which has the value -1 at the index (i, i) and 1 at the index $(i, i + 1)$ and all the other values are zero at the row i . For each direction vector $\mathbf{d} = \Delta E d_s$ with some ΔE , the directional derivative is calculated by $\mathbf{d}^T \nabla C(\mathbf{E})$. After finding the direction for the maximum increase, the energy transfer \mathbf{d} is applied. The transfer continues until no further increase in the capacity is observed. The same iteration is

Algorithm 2: Gradient Descent Scheduling Algorithm

```

while  $\Delta E >= \Delta E_{Thr}$  do
 $\Delta E = \Delta E/2$ ;
while The increase in capacity  $C(E)$  is above some threshold do
for all  $nodenum = 1$  to  $2$  do
Compute the gradient for energy transfers of the  $nodenum$ 
Find the direction  $d$  for the maximum directional derivative and perform
the energy scheduling
Compute the increase in the capacity  $C(E)$ 
end for
end while
end while
end while

```

TABLE I
THE GLOBAL VALUES USED IN NUMERICAL SIMULATIONS

Parameter	Meaning	Value
W_{Tot}	Total bandwidth	1 MHz
N_0	Noise	10^{-19} W/Hz
h	(Path Loss)	10^{-11}
E_1	First user harvested energies	[3 6 10] mJ
E_2	Second user harvested energies	[4 11 6] mJ
t_1	First user harvesting times	[0 2 6] seconds
t_2	Second user harvesting times	[0 5 8] seconds
T_f	Final time	11
A	Constant	$N_0 W_{Tot} / h = 0.01$
N	Number of time intervals	5

then repeated for the second node. The iterations continue by decreasing ΔE incrementally until below some threshold ΔE_{Thr} . The algorithm is presented in Algorithm-2. Since the algorithm computes all the possibilities, it is expected to converge to the global optimum. This method is compared with the performance of the water filling algorithm.

V. NUMERICAL SIMULATION RESULTS

In this section, the proposed solutions and the algorithms are numerically simulated for parameters shown in Table I. The users harvest energy at 3 time instants at the specified time instants. Furthermore, the constraint for the total received energy is not simulated and left as a future work, i.e., λ_8 in (34), (38), (42 - 44), (48 - 54) is taken as zero. In Fig. 3, the scatter plot of the capacity boundary at the final time T_f is shown for both the water filling algorithm and the gradient descent search algorithm. It can be observed that they form almost the same surface proving the optimality of both the methods. The surface formed from the scattered points is shown in Fig. 4 which resembles the capacity boundary surface for the single time interval as shown in Fig. 2. Furthermore, the comparison between the surfaces formed from the scatter plots of the water filling and the gradient descent search algorithm is shown in Fig. 5. The surfaces are formed for specific (R_1, R_2) pairs and the corresponding R_0 is compared. It is observed that they give almost the same values except the limiting regions where R_0 decays to zero due to the finite number of μ_1, μ_2, μ_0 samples. The water filling behaviour and the power consumption profiles of the users are seen in Figs. 6-9 for various regions corresponding to (μ_1, μ_2, μ_0) . As shown in Fig. 6, when $\mu_1 \geq \mu_2 \geq \mu_0$ with μ_0 comparable

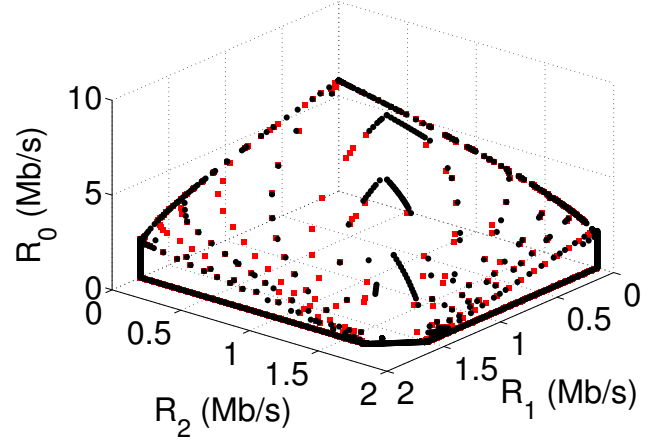


Fig. 3. Capacity boundary surface scatter plot formed by choosing various μ_1, μ_2 and μ_3 by using the water filling algorithm (black) and the gradient descent search algorithm (red).

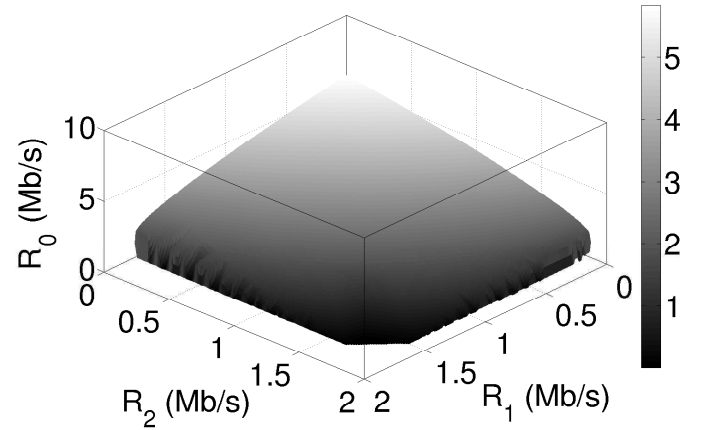


Fig. 4. The capacity boundary surface formed from the scatter plot points in Fig. 3.

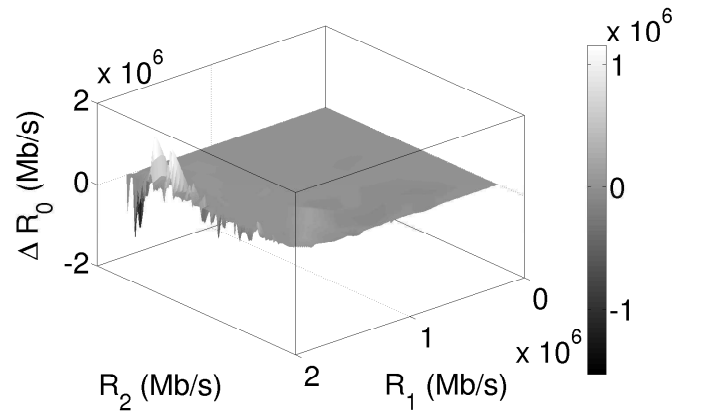


Fig. 5. The comparison between the capacity boundary surfaces formed from the scatter plots of the water filling and the gradient descent search algorithm.

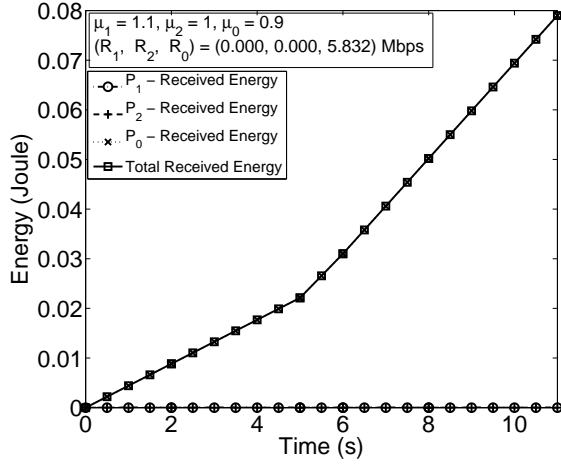


Fig. 6. Received energy for each message and the received total energy for $(\mu_1 = 1.1, \mu_2 = 1, \mu_0 = 0.9)$ comparable to μ_1 and μ_2 or $\mu_0 \geq \max(\mu_1, \mu_2)$.

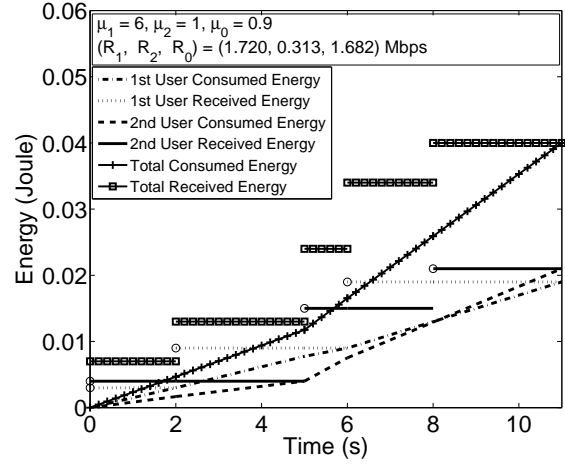


Fig. 8. Consumed and harvested energies for each user and for the total, for $(\mu_1 = 6, \mu_2 = 1, \mu_0 = 0.9)$ with $\mu_1 \gg \mu_2, \mu_0$ and μ_0 comparable to μ_2 .

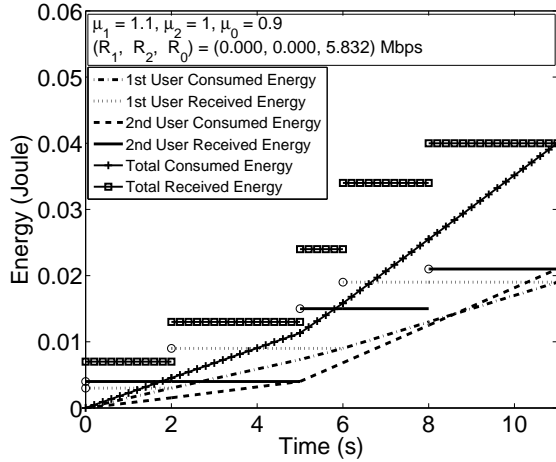


Fig. 7. Consumed and harvested energies for each user and for the total, for $(\mu_1 = 1.1, \mu_2 = 1, \mu_0 = 0.9)$ with μ_0 comparable to μ_1 and μ_2 or $\mu_0 \geq \max(\mu_1, \mu_2)$.

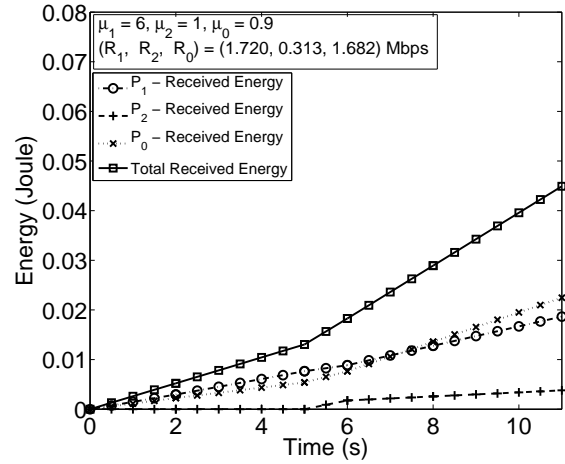


Fig. 9. Received energy for each message and the received total energy for $(\mu_1 = 6, \mu_2 = 1, \mu_0 = 0.9)$ with $\mu_1 \gg \mu_2, \mu_0$ and μ_0 comparable to μ_2 .

to μ_1 and μ_2 or $\mu_0 \geq \max(\mu_1, \mu_2)$, all the power is consumed for the common data which leads to the maximum received total energy and the rate R_0 . In Fig. 7, the consumed and the harvested energies for each user are shown with the total received and the consumed energy. It can be observed that the individual and the total energy profiles are similar to the single user power consumption profile defined in [5]. If μ_1 is further increased compared with μ_2 and μ_0 , the consumed energy profile for each user and for the total do not change too much as shown in Fig. 8. However, as μ_1 increases, most of the energy goes to the messages W_1 and W_0 as shown in Fig. 9 while the total received energy is decreased.

VI. CONCLUSION

In this paper, optimum offline packet scheduling and energy consumption policy is developed for 2-user Gaussian MAC with common data scheme. KKT solution is presented and

a water filling algorithm is presented achieving the optimum solution. The water filling algorithm includes 3-level water filling and specific complicated structure due to the regional behaviour of KKT multipliers in Gaussian MAC with common data. In the offline modelling and solution of the packet scheduling problem, the constraint of the total received energy is taken into account. Optimum water filling algorithm is compared with the gradient descent search algorithm which gives the global optimum solution. It is observed that both solutions are very close and optimal. In addition, the capacity boundary region for the individual and common data rates are obtained with simulations of the optimum solution and various points on the surface of the capacity boundary are compared. The fundamentals of the optimal packet scheduling for the MAC scheme with common data is established which can improve the performance of WSNs where highly correlated data exists. Finally, the effect of the total received power constraint and the extension of the work to both data and

energy transfer are left as a future work.

APPENDIX A KKT MULTIPLIER REGIONS AND SOLUTIONS

The following definitions are used next, $g \equiv g(\lambda_1, \lambda_2, \lambda_8)$, $\alpha \equiv (\mu_2 - \mu_0) / (\lambda_2 - g)$, $\beta \equiv (\mu_1 - \mu_2) / (\lambda_1 - \lambda_2)$, $\gamma \equiv (\mu_0 - \mu_1)(g - \lambda_1)$. The regions are defined for varying (λ_1, λ_2) with the corresponding solutions. R_1 refers to the case where the power values are 0 and skipped in the solutions. R_i refers the region, and S_i refers the solution in that region.

For the first case, i.e., $\mu_1 \geq \mu_2 \geq \mu_0$, the KKT multiplier regions and solutions for the power variables are the following,

$$R_1 = \left\{ \mu_i < \lambda_i : i \in [1, 2], g > \mu_0 \right\} \quad (61)$$

$$R_2 = \left\{ \mu_i - \mu_0 + g < \lambda_i : i \in [1, 2], \frac{\mu_0}{g} > 1 \right\} \quad (62)$$

$$R_3 = \left\{ \mu_1 > \lambda_1, \frac{g}{\lambda_1} > \frac{\mu_0}{\mu_1}, \frac{\lambda_2}{\lambda_1} > \frac{\mu_2}{\mu_1} \right\} \quad (63)$$

$$R_4 = \left\{ \mu_1 - \mu_2 < \lambda_1 - \lambda_2, \frac{g}{\lambda_2} > \frac{\mu_0}{\mu_2}, \lambda_2 < \mu_2 \right\} \quad (64)$$

$$R_5 = \left\{ \frac{\mu_0}{g} > 1, \gamma > \alpha, P_{0,1} > 0 \right\} \quad (65)$$

$$R_6 = \left\{ \frac{\mu_0}{g} > 1, \frac{\lambda_1 - \lambda_2}{\mu_1 - \mu_2} > 1, \alpha > 1, P_0 > 0 \right\} \quad (66)$$

$$R_7 = \left\{ \frac{g}{\lambda_2} > \frac{\mu_0}{\mu_2}, \frac{\mu_2}{\lambda_2} > 1, \frac{\lambda_2}{\lambda_1} < \frac{\mu_2}{\mu_1}, P_1 > 0 \right\} \quad (67)$$

$$R_8 = \left\{ \frac{\mu_0}{g} > \beta > 1, \alpha > 1, P_{0,2} > 0 \right\} \quad (68)$$

$$S_2 : P_0 = \frac{\mu_0}{g} - 1, P_{1,2} = 0 \quad (69)$$

$$S_3 : P_1 = \frac{\mu_1}{\lambda_1} - 1, P_{0,2} = 0 \quad (70)$$

$$S_4 : P_2 = \frac{\mu_2}{\lambda_2} - 1, P_{0,1} = 0 \quad (71)$$

$$S_5 : P_1 = \gamma - 1; P_0 = \frac{\mu_0}{g} - P_1 - 1 \quad (72)$$

$$S_6 : P_2 = \alpha - 1; P_0 = \frac{\mu_0}{g} - P_2 - 1, P_1 = 0 \quad (73)$$

$$S_7 : P_1 = \frac{\mu_1 - \mu_2}{\lambda_1 - \lambda_2} - 1; P_2 = \frac{\mu_2}{\lambda_2} - P_1 - 1, P_0 = 0 \quad (74)$$

$$S_8 : P_1 = \frac{\mu_1 - \mu_2}{\lambda_1 - \lambda_2} - 1; P_2 = \frac{\mu_2 - \mu_0}{\lambda_2 - g} - P_1 - 1; \quad (75)$$

$$P_0 = \frac{\mu_0}{g} - \frac{\mu_2 - \mu_0}{\lambda_2 - g} \quad (76)$$

For the second case, i.e., $\mu_1 \geq \mu_0 \geq \mu_2$, the following regions and the solutions are satisfied,

$$R_1 = \left\{ \mu_1 < \lambda_1, g > \mu_0 \right\}; R_2 = \left\{ \mu_1 > \lambda_1, \frac{g}{\lambda_1} > \frac{\mu_0}{\mu_1} \right\} \quad (77)$$

$$R_3 = \left\{ \frac{1}{\gamma} > 1, \frac{\mu_0}{g} > 1 \right\}; R_4 = \left\{ \frac{\mu_0}{g} > 1, P_{0,1} > 0 \right\} \quad (78)$$

$$S_2 : P_1 = \frac{\mu_1}{\lambda_1} - 1, P_{0,2} = 0; S_3 : P_0 = \frac{\mu_0}{g} - 1, P_{1,2} = 0 \quad (79)$$

$$S_4 : P_1 = \frac{\mu_1 - \mu_0}{\lambda_1 - g} - 1, P_0 = \frac{\mu_0}{g} - P_1 - 1, P_2 = 0 \quad (80)$$

For the case of $\mu_0 \geq \max(\mu_1, \mu_2)$, the solution is given by $P_0 = \frac{\mu_0}{g} - 1$.

APPENDIX B COMPARISON TABLE OF WATER LEVELS

Let us define $g(j) \triangleq g(\lambda_{1,j}^p, \lambda_{2,j}^p, \lambda_8)$. Then, for the case $\mu_1 \geq \mu_2 \geq \mu_0$, 3 water levels to be compared are the following,

$$W_1 = \frac{\mu_0}{1 + P_1 + P_2 + P_0} + \frac{\mu_2 - \mu_0}{1 + P_1 + P_2} + \frac{\mu_1 - \mu_2}{1 + P_1} \quad (81)$$

$$W_2 = \frac{\mu_0}{1 + P_1 + P_2 + P_0} + \frac{\mu_2 - \mu_0}{1 + P_1 + P_2} \quad (82)$$

$$W_3 = \frac{\mu_0}{1 + P_1 + P_2 + P_0} \quad (83)$$

while for the case $\mu_1 \geq \mu_0 \geq \mu_2$, 2 water levels to be compared are the following,

$$W_1 = \frac{\mu_0}{1 + P_1 + P_0} + \frac{\mu_1 - \mu_0}{1 + P_1}; W_2 = \frac{\mu_0}{1 + P_1 + P_0} \quad (84)$$

and finally, for the case $\mu_0 \geq \max(\mu_1, \mu_2)$, the water level to be compared is $W_1 = \frac{\mu_0}{1 + P_0}$. The water levels and the regions for these cases are shown in Table II.

For different optimized regions in the neighbouring time intervals n and $n - 1$, with respect to the specific node transferring energy, the equalities/inequalities to be satisfied for the optimum solutions are seen in Table III for the case $\mu_1 \geq \mu_2 \geq \mu_0$ where the first node transfers energy and in Table IV where the second node transfers energy. The cases for $\mu_1 \geq \mu_0 \geq \mu_2$ and $\mu_0 \geq \max(\mu_1, \mu_2)$ are not shown due to space limitations.

TABLE II
THE KKT MULTIPLIER REGIONS AND THE WATER LEVELS FOR TIME STEP j FOR VARYING (μ_1, μ_2, μ_0)

$\mu_1 \geq \mu_2 \geq \mu_0$	R_2	R_3	R_4	R_5	R_6	R_7	R_8
P_1	0	> 0	0	> 0	0	> 0	> 0
P_2	0	0	> 0	0	> 0	> 0	> 0
P_0	> 0	0	0	> 0	> 0	0	> 0
W_1	$\lambda_{1,j}^p - \lambda_{5,j}$	$\lambda_{1,j}^p$	$\lambda_{1,j}^p - \lambda_{5,j}$	$\lambda_{1,j}^p$	$\lambda_{1,j}^p - \lambda_{5,j}$	$\lambda_{1,j}^p$	$\lambda_{1,j}^p$
W_2	$\lambda_{2,j}^p - \lambda_{6,j}$	$\lambda_{2,j}^p - \lambda_{6,j}$	$\lambda_{2,j}^p$	$\lambda_{2,j}^p - \lambda_{6,j}$	$\lambda_{2,j}^p$	$\lambda_{2,j}^p$	$\lambda_{2,j}^p$
W_3	$g(j)$	$g(j) - \lambda_{7,j}$	$g(j) - \lambda_{7,j}$	$g(j)$	$g(j)$	$g(j) - \lambda_{7,j}$	$g(j)$
$\mu_1 \geq \mu_0 \geq \mu_2$	R_2	R_3	R_4			$\mu_0 \geq \max(\mu_1, \mu_2)$	R_2
P_1	0	> 0	> 0			P_1	0
P_2	0	0	0			P_2	0
P_0	> 0	0	> 0			P_0	> 0
W_1	$\lambda_{1,j}^p - \lambda_{5,j}$	$\lambda_{1,j}^p$	$\lambda_{1,j}^p$			W_1	$g(j)$
W_2	$g(j)$	$g(j) - \lambda_{7,j}$	$g(j)$				

TABLE III

THE KKT MULTIPLIER REGIONS AND THE OPTIMALITY CONDITIONS FOR TIME STEPS j AND $j + 1$ WHEN THE 1ST NODE TRANSFERS ENERGY, $\mu_1 \geq \mu_2 \geq \mu_0$

		$W_1(j + 1)$	
		$R_{2,4,6}$	$R_{3,5,7,8}$
$W_1(j)$	$R_{2,4,6}$	x	\leq
	$R_{3,5,7,8}$	\geq	$=$
		$W_2(j + 1)$	
		$R_{2,3,4,5,6,7,8}$	
$W_2(j)$	$R_{2,3,5}$	x	
	$R_{4,6,7,8}$	\geq	
		$W_3(j + 1)$	
		$R_{2,3,4,5,6,7,8}$	
$W_3(j)$	$R_{2,5,6,8}$	\geq	
	$R_{3,4,7}$	x	

TABLE IV

THE KKT MULTIPLIER REGIONS AND THE OPTIMALITY CONDITIONS FOR TIME STEPS j AND $j + 1$ WHEN THE 2ND NODE TRANSFERS ENERGY, $\mu_1 \geq \mu_2 \geq \mu_0$

		$W_1(j + 1)$	
		$R_{2,3,4,5,6,7,8}$	
$W_1(j)$	$R_{2,3,5}$	x	
	$R_{4,6,7,8}$	\geq	
		$W_2(j + 1)$	
		$R_{2,3,5}$	$R_{4,6,7,8}$
$W_2(j)$	$R_{2,3,5}$	x	\leq
	$R_{4,6,7,8}$	\geq	$=$
		$W_3(j + 1)$	
		$R_{2,3,4,5,6,7,8}$	
$W_3(j)$	$R_{2,5,6,8}$	\geq	
	$R_{3,4,7}$	x	

REFERENCES

[1] J. Yang and S. Ulukus, "Optimal packet scheduling in a multiple access channel with rechargeable nodes," *IEEE International Conference on Communications (ICC)*, pp. 1–5, 2011.

[2] J. Yang and S. Ulukus, "Optimal packet scheduling in a multiple access channel with energy harvesting transmitters," *Journal of Communications and Networks*, vol. 14, no. 2, pp. 140–150, 2012.

[3] M. B. Khuzani and P. Mitran, "On online energy harvesting in multiple access communication systems," *Arxiv preprint arXiv:1301.1027v2*, 2013.

[4] K. Tutuncuoglu and A. Yener, "The energy harvesting multiple access channel with energy storage losses," *IEEE Information Theory Workshop (ITW)*, pp. 94–98, 2012.

[5] J. Yang and S. Ulukus, "Optimal packet scheduling in an energy harvesting communication system," *IEEE Transactions on Communications*, vol. 60, no. 1, pp. 220–230, 2012.

[6] J. Yang and S. Ulukus, "Transmission completion time minimization in an energy harvesting system," *IEEE 44th Annual Conference on Information Sciences and Systems (CISS)*, pp. 1–6, 2010.

[7] O. Ozel et al., "Transmission with energy harvesting nodes in fading wireless channels: Optimal policies," *IEEE Journal on Selected Areas in Communications*, vol. 29, no. 8, pp. 1732–1743, 2011.

[8] B. Gurakan et al., "Energy cooperation in energy harvesting wireless communications," *IEEE International Symposium on Information Theory Proceedings (ISIT)*, pp. 965–969, 2012.

[9] B. Prabhakar, E.U. Biyikoglu and A. E. Gamal, "Energy-efficient transmission over a wireless link via lazy packet scheduling," *Proceedings of IEEE INFOCOM*, pp. 386–394, 2001.

[10] O. Kaya and S. Ulukus, "Achieving the capacity region boundary of fading CDMA channels via generalized iterative waterfilling," *IEEE Transactions on Wireless Communications*, vol. 5, no. 11, pp. 3215–3223, 2006.

[11] B. Gurakan et al., "Two-way and multiple-access energy harvesting systems with energy cooperation," *IEEE Forty Sixth Asilomar Conference on Signals, Systems and Computers (ASILOMAR)*, pp. 58–62, 2012.

[12] O. Ozel and S. Ulukus, "On the capacity region of the Gaussian MAC with batteryless energy harvesting transmitters," *IEEE Global Communications Conference (GLOBECOM)*, pp. 2385–2390, 2012.

[13] K. Tutuncuoglu and A. Yener, "Communicating with energy harvesting transmitters and receivers," *IEEE Information Theory and Applications Workshop (ITA)*, pp. 240–245, 2012.

[14] M. C. Vuran, O. B. Akan and I. F. Akyildiz, "Spatio-temporal correlation: theory and applications for wireless sensor networks," *Computer Networks*, vol. 45, no. 3, pp. 245–259, 2004.

[15] B. Gulbahar and O. B. Akan, "Information theoretical optimization gains in energy adaptive data gathering and relaying in cognitive radio sensor networks," *IEEE Transactions on Wireless Communications*, vol. 11, no. 5, pp. 1788–1796, 2012.

[16] N. Liu and S. Ulukus, "Capacity region and optimum power control strategies for fading Gaussian multiple access channels with common data," *IEEE Transactions on Communications*, vol. 54, no. 10, pp. 1815–1826, 2006.

[17] A. Hagni et al., "The capacity region of p-transmitter/q-receiver multiple-access channels with common information," *IEEE Transactions on Information Theory*, vol. 57, no. 11, pp. 7359–7376, 2011.

[18] R. Rajesh and V. Sharma, "Joint source-channel coding over a fading multiple access channel with partial channel state information," *IEEE Global Telecommunications Conference (GLOBECOM)*, pp. 1–7, 2009.

[19] R. K. Farsani and F. Marvasti, "Multiple Access Channels with Cooperative Encoders and Channel State Information," *arXiv preprint arXiv:1009.6008*, 2010.

[20] A.M. Fouladgar and O. Simeone, "On the transfer of information and energy in multi-user systems," *IEEE Communications Letters*, vol. 16, no. 11, pp. 1733–1736, 2012.

[21] P. Popovski and O. Simeone, "Two-way communication with energy exchange," *IEEE ITW*, pp. 592–596, 2012.

[22] K. Tutuncuoglu and A. Yener, "Multiple access and two-way channels with energy harvesting and bi-directional energy cooperation," *IEEE Information Theory and Applications Workshop (ITA)*, pp. 1–8, 2013.

[23] K. Tutuncuoglu and A. Yener, "Cooperative energy harvesting communications with relaying and energy sharing," *IEEE Information Theory Workshop (ITW)*, pp. 1–5, 2013.